# Isotope branching and tunneling in $O(^3P)+HD \rightarrow OH+D$; $OD+H$ reactions

Renat A. Sultanov[a] and N. Balakrishnan[b]
*Department of Chemistry, University of Nevada Las Vegas, Las Vegas, Nevada 89154*

(Received 4 August 2004; accepted 7 September 2004)

The $O(^3P)+HD$ and $O(^3P)+D_2$ reactions are studied using quantum scattering calculations and chemically accurate potential energy surfaces developed for the $O(^3P)+H_2$ system by Rogers *et al.* [J. Phys. Chem. A **104**, 2308 (2000)]. Cross sections and rate coefficients for OH and OD products are calculated using accurate quantum methods as well as the *J*-shifting approximation. The *J*-shifting approach is found to work remarkably well for both $O+HD$ and $O+D_2$ collisions. The reactions are dominated by tunneling at low temperatures and for the $O+HD$ reaction the hydrogen atom transfer leading to the OH product dominates at low temperatures. Our result for the OH/OD branching ratio is in close agreement with previous calculations over a wide range of temperatures. The computed OH/OD branching ratios are also in close agreement with experimental results of Robie *et al.* [Chem. Phys. Lett. **134**, 579 (1987)] at temperatures above 400 K but the theoretical results do not reproduce the rapid rise in the experimental values of the branching ratio for temperatures lower than 350 K. We believe that new measurements could resolve the long-standing discrepancy between experiment and theory for this benchmark reaction. © *2004 American Institute of Physics.* [DOI: 10.1063/1.1810478]

## I. INTRODUCTION

The issue of tunneling in chemical reactions has received important attention over the years. Most reactions between neutral atoms and molecules involve an energy barrier and occur mainly by tunneling at low temperatures. One example of a reaction where tunneling is thought to play an important role is the $O(^3P)+HD$ reaction[1–11] which yields $OH+D$ or $OD+H$ products,

$$O+HD \xrightarrow{k_{HD}} OH+D \tag{1}$$

and

$$O+DH \xrightarrow{k_{DH}} OD+H, \tag{2}$$

and the ratio $k_{HD}/k_{DH}$ is referred to as the intramolecular kinetic isotope effect (KIE). Robie *et al.*[6,9] reported experimental measurements of $k_{HD}/k_{DH}$ using laser-induced fluorescence techniques and found a very strong negative temperature dependence for the KIE. While transition-state theory calculations which do not include tunneling[1,3] failed to account for the observed temperature dependence, calculations that accounted for tunneling[1,3] predicted strong negative temperature dependence and were partially successful in explaining the observed isotope effect. For example, between 500 and 370 K, collinear exact quantum calculation[5] and tunneling corrected transition-state theories[7] predicted branching ratios in the range of 7.2–7.4, in close agreement with experimental data.[6,9] However, at temperatures between 350 and 300 K the experimental KIE showed a steep increase which was not reproduced by theoretical calculations. The discrepancy between experiment and theory was considered to be genuine and Robie *et al.*[9] concluded that the sources of the difference were inaccuracies in the potential surfaces used. Subsequent calculations by Joseph, Truhlar, and Garrett[7] using improved potential energy surfaces (PESs) and variational transition-state theories with tunneling correction were also unable to reproduce the experimental results for temperatures lower than 350 K.

The $O+H_2$ and its isotopic counterparts have been the topics of a large number of theoretical[12–26] and experimental studies.[27–31] Recently, there has been renewed interest in the $O+H_2$ reaction, driven partly by its importance in atmospheric and combustion chemistry[22,25,32] and partly by new measurements.[21] The reaction occurs by a hydrogen abstraction mechanism and is an elementary step in the combustion hydrocarbons. On the theoretical side, chemically accurate potential energy surfaces of $^3A'$ and $^3A''$ symmetry have been reported by Rogers *et al.*[19] and accurate quantum calculations of the $O+H_2$ reaction employing these surfaces have been carried out.[21,22,25,26] Furthermore, the first crossed molecular beam study of the $O+H_2$ reaction was reported in 2003 by Garton *et al.*[21] and quantum calculations[21,22,25,26] employing the potential surfaces of Rogers *et al.* quantitatively reproduce the experimental results. In light of the long-standing discrepancy between theory and experiment on the KIE in $O+HD$ reaction, we believe that the recent developments on the $O+H_2$ system provide an excellent basis for revisiting the $O+HD$ reaction.

In this paper, we report quantum mechanical investigations of the $O+HD$ and $O+D_2$ reactions using the chemically accurate potential energy surfaces of Rogers *et al.*[19] While our results for KIE in $O+HD$ reaction agree with previous theoretical results they do not reproduce the dramatic increase observed in experiments at temperatures below 350 K.

[a]Electronic mail: sultano2@unlv.nevada.edu
[b]Author to whom correspondence should be addressed. Fax: 702-895-4072. Electronic mail: naduvala@unlv.nevada.edu

 

The paper is organized as follows: In Sec. II we give a brief description of the methodology. Results of our calculations are given in Sec. III and a summary of our findings is given in Sec. IV.

## II. METHOD

The reactive scattering calculations are carried out in hyperspherical coordinates using the *ABC* program[33] of Manolopoulos and co-workers. Initial-state-selected cross sections corresponding to vibrational-rotational levels $(vj)$ at an incident kinetic energy $E_{\rm kin}$ are computed using the formula,

$$\sigma_{vj}(E_{\rm kin})=\frac{\pi}{k_{vj}^2(2j+1)}\sum_{J=0}^{\infty}(2J+1)P_{vj}^{J}(E_{\rm kin}), \tag{3}$$

where $k_{vj}$ is the wave vector for the incident channel, $J$ is the total angular momentum quantum number, and $P_{vj}^{J}(E_{\rm kin})$ are initial-state-selected reaction probabilities given by

$$P_{vj}^{J}(E_{\rm kin})=\sum_{v'j'k'k}|S_{v'j'k',vjk}^{J}(E_{\rm kin})|^2, \tag{4}$$

where $S_{v'j'k',vjk}^{J}(E_{\rm kin})$ is an element of the $S$-matrix. The angular momentum projection quantum numbers $k$ and $k'$ are restricted to values $0\leqslant k\leqslant \min(J,j)$ and $0\leqslant k'\leqslant \min(J,j')$. Initial-state-selected rate constants are obtained by averaging the corresponding cross sections over a Boltzmann distribution of relative speeds of the colliding partners,

$$k_{vj}(T)=\frac{1}{g}\sqrt{\frac{8k_BT}{\pi\mu}}\int_0^{\infty}\frac{1}{(k_BT)^2}\sigma_{vj}(E_{\rm kin})\times e^{-E_{\rm kin}/k_BT}E_{\rm kin}dE_{\rm kin}, \tag{5}$$

where $g=3$ is the electronic degeneracy,[14] $\mu$ is the reduced mass of the atom-molecule system, $T$ is the temperature, and $k_B$ is the Boltzmann constant.

For an exact description of the dynamics, one needs to perform calculations for all contributing values of the total angular momentum quantum number $J$. Such calculations are practical for only a relatively few systems due to the large number of coupled channels to be included. For the $O+H_2(v=0,j=0)$ system, we have performed such exact quantum calculations[26] and it was shown that one can obtain accurate results using the much simpler $J$-shifting approximation.[34] Here, we will first test the adequacy of the $J$-shifting approximation by performing full quantum calculations in a limited range of energies where quantum effects are the most important. The $J$-shifting approach assumes that the reaction takes place through a transition state and that the rotational energy $E_J^{\ddagger}$ of the triatomic $[OHD]^{\ddagger}$ species is not available to overcome the transition state. The advantage of the $J$-shifting approximation is that one needs to compute probabilities for only the $J=0$ case. Cross sections for $J>0$ are obtained from the $J=0$ result by $J$-shifting,

$$\tilde{\sigma}_{vj}(E_{\rm kin})=\frac{\pi}{k_{vj}^2(2j+1)}\sum_{J=0}^{\infty}(2J+1)P_{vjJ}^{\ddagger}(E_{\rm kin}), \tag{6}$$

where the reaction probabilities $P_{vjJ}^{\ddagger}(E_{\rm kin})$ are calculated from the corresponding $J=0$ values according to

$$P_{vjJ}^{\ddagger}(E_{\rm kin})=P_{vjJ=0}(E_{\rm kin}-E_J^{\ddagger}). \tag{7}$$

For the present system, the transition state is linear in geometry and $E_J^{\ddagger}=B^{\ddagger}J(J+1)$, where $B^{\ddagger}$ is the rotational constant of the transition-state species.

To obtain thermal rate coefficients one needs to average over a thermal populations of rotational and vibrational levels,

$$k(T)=\frac{\Sigma_{vj}^{\infty}(2j+1)k_{vj}(T)e^{-E_{vj}/k_BT}}{Q_{\rm rot}(T)Q_{\rm vib}(T)}, \tag{8}$$

where $E_{vj}$ are rovibrational energy levels of the molecule and $Q_{\rm rot}$ and $Q_{\rm vib}$ are, respectively, the rotational and vibrational partition functions of the molecule. A more convenient expression for the thermal rate coefficient involves Boltzmann averaging of the cumulative reaction probability (CRP) (Refs. 35 and 36),

$$k(T)=\frac{1}{2\pi\hbar Q_{\rm mol}(T)}\int_{-\infty}^{+\infty}e^{-E/k_BT}N(E)dE, \tag{9}$$

where $E$ is the total energy and $Q_{\rm mol}(T)$ is molecular reactant partition function: $Q_{\rm mol}(T)=Q_{\rm el}(T)Q_{\rm vib}(T)Q_{\rm rot}(T)\times Q_{\rm trans}(T)$, where $Q_{\rm el}(T)$ and $Q_{\rm trans}(T)$ are, respectively, the electronic and translational partition functions. For the present system, $Q_{\rm el}(T)=3$. The cumulative reaction probability $N(E)$ is given by

$$N(E)=\sum_{J=0}^{\infty}(2J+1)N_J(E), \tag{10}$$

where $N^J(E)=\Sigma_{vj}P_{vj}^{J}(E)$. The $J$-dependent CRP values $N_J(E)$ are also obtained using the $J$-shifting approximation:

$$N_J(E)\approx N_{J=0}(E-E_J^{\ddagger}). \tag{11}$$

With the $J$-shifting approximation, the final expression for the thermal rate coefficient becomes

$$k(T)=\frac{Q_{\rm rot}^{\ddagger}(T)}{2\pi\hbar Q_{\rm mol}(T)}\int_{-\infty}^{+\infty}e^{-E/k_BT}N_{J=0}(E)dE, \tag{12}$$

where $Q_{\rm rot}^{\ddagger}(T)$ is the rotational partition function of the transition-state complex:

$$Q_{\rm rot}^{\ddagger}(T)=\sum_{J=0}^{\infty}(2J+1)e^{-E_J^{\ddagger}/k_BT}\approx k_BT/B^{\ddagger}. \tag{13}$$

## III. RESULTS AND DISCUSSION

### A. O($^3P$)+HD reaction

Quantum calculations of the O+HD reaction is much more challenging than that of the $O+H_2$ or $O+D_2$ reactions due to the presence of three different atoms and hence three distinct arrangement channels. A large number of test calculations have been carried out to secure convergence of the results with respect to all parameters that enter into the numerical solution of the Schrödinger equation. This includes the cutoff energy $E_{\rm max}$ and the maximum value of the rotational quantum number $j_{\rm max}$ in each channel which deter-

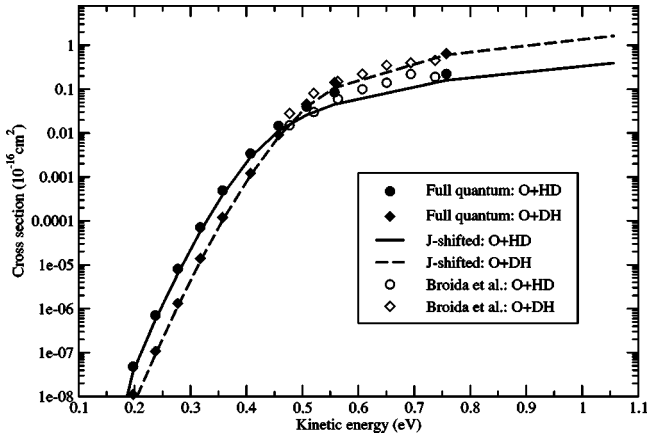


FIG. 1. Initial-state-selected cross sections $\sigma_{vj}(E_{\mathrm{kin}})$ for $\mathrm{O}+\mathrm{DH}(v=0,j=0)$ and $\mathrm{O}+\mathrm{HD}(v=0,j=0)$ reactions from the full quantum calculation, the $J$-shifting approximation, and QCT calculations of Broida and Persky (Ref. 16) as functions of the kinetic energy. Results are for the $^3A''$ PES.

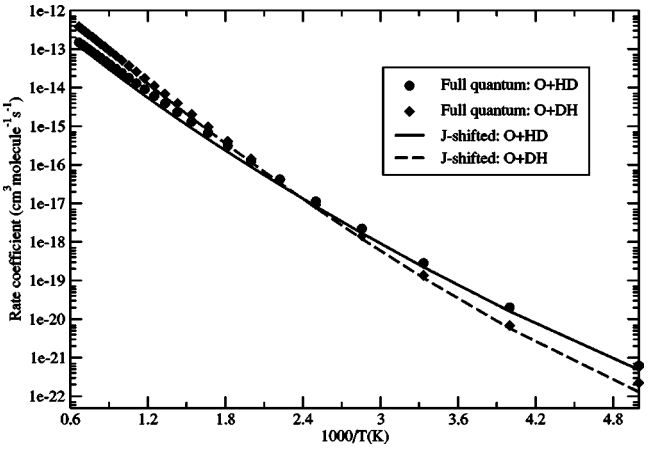


FIG. 2. Initial-state-selected rate coefficients $k_{vj}(T)$ for $\mathrm{O}+\mathrm{DH}(v=0,j=0)$ and $\mathrm{O}+\mathrm{HD}(v=0,j=0)$ reactions from the full quantum calculation and those obtained using the $J$-shifting approximation for collisions occurring on the $^3A''$ PES as functions of the temperature.

mine the number of rovibrational levels of the reactant and product molecules to be included in the close-coupled equations. Values of $E_{\max}=3.2$ eV and $j_{\max}=22$ were used in the calculations reported here which result in a total of 498 channels for $J=0$. The number of channels $N$ quickly escalates for higher values of $J$ with $N=971$ and 1419, respectively, for $J=1$ and 2, which makes full quantum calculations for higher values of $J$ prohibitively expensive. To facilitate calculations for $J>0$ we have used a cutoff value of $k_{\max}=4$ for calculations involving $J>4$. This is a good approximation because the reaction is collinearly dominated and only the first few values of $k$ significantly contribute to the reaction. For the integration over the hyperradius we used $\rho_{\min}=0.1a_0$, $\rho_{\max}=27.0a_0$, and $\Delta\rho=0.05a_0$.

The main objective of the study is to calculate the branching ratio between the OH and OD product channels in the $\mathrm{O}+\mathrm{HD}$ reaction. The discrepancy between theoretical and experimental values of the branching ratio occurs for temperatures less than 400 K. In this temperature range almost all contributions to the rate coefficients arise from cross sections at kinetic energies lower than 0.75 eV. Thus, to reduce the computational cost we restrict the full quantum calculations for kinetic energies lower than 0.75 eV.

We first establish the accuracy of the $J$-shifting approximation by comparing with results from the full quantum calculation. This is shown in Fig. 1, where we compare cross sections for the two branches obtained from the full quantum calculation and the $J$-shifting approximation on the $^3A''$ potential. Also included in Fig. 1 are the quasiclassical trajectory (QCT) calculation of Broida and Persky[16] using the PES of Johnson and Winter.[12] It is seen that the $J$-shifting approximation quantitatively reproduces results from the full quantum calculation. The agreement is similar to that of the $\mathrm{O}+\mathrm{H_2}$ reaction for which we have reported[25,26] numerically exact calculations for kinetic energies up to 1.0 eV which required $J$ values up to 40 in Eq. (3) in securing convergence of the cross sections. The full quantum calculations presented here include $J$ values up to 30. It is also interesting to note that the cross sections for the hydrogen atom transfer reaction leading to the $\mathrm{OH}+\mathrm{D}$ product dominates at energies lower than 0.4 eV, demonstrating the importance of tunneling in the reaction. At energies above 0.5 eV, tunneling is less important and the $\mathrm{OD}+\mathrm{H}$ channel dominates. The QCT results, while in good agreement with the quantum results, are not available in the tunneling regime, but they reproduce the major features of the quantum results, including the product branching, at higher energies.

In Fig. 2 we compare rate coefficients for the $\mathrm{O}+\mathrm{HD}(v=0,j=0)$ reaction on the $^3A''$ potential evaluated using the full quantum method and the $J$-shifting calculations. It is seen that the results are in excellent agreement and that the $J$-shifting method can be used to obtain rate coefficients without loosing accuracy and with orders of magnitude of lower computational cost. The transition states of the $\mathrm{O}+\mathrm{H_2}/\mathrm{HD}/\mathrm{DH}/\mathrm{D_2}$ reactions are linear. In Table I, we give the rotational constants used in evaluating the rotational energies of the transition-state species for the $J$-shifting method. For completeness, we also include results for $\mathrm{O}+\mathrm{H_2}$.

Rate coefficients are obtained by adding contributions from the $^3A'$ and $^3A''$ potentials. Since major contribution to the rate coefficient arises from the $^3A''$ potential[22] and that the $J$-shifting approximation works so well, we have not repeated the full calculations on the $^3A'$ potential. Instead, we use the $J$-shifting approximation to obtain cross sections on the $^3A'$ potential. Figure 3 shows $J$-shifted cross sections for the two branches of the $\mathrm{O}+\mathrm{HD}(v=0,j=0)$ reaction obtained using the $^3A'$ and $^3A''$ PESs. Rate coefficients for the $\mathrm{O}+\mathrm{HD}(v=0,j=0)$ reaction in the temperature range 200–1000 K obtained using the $J$-shifting approximation are given in Table II.

TABLE I. Rotational constants $B^{\ddagger}$ ($\mathrm{cm}^{-1}$) of the $[\mathrm{O}\cdots\mathrm{H}\cdots\mathrm{H}]^{\ddagger}$, $[\mathrm{O}\cdots\mathrm{H}\cdots\mathrm{D}]^{\ddagger}$, $[\mathrm{O}\cdots\mathrm{D}\cdots\mathrm{H}]^{\ddagger}$, and $[\mathrm{O}\cdots\mathrm{D}\cdots\mathrm{D}]^{\ddagger}$ transition-state species for the two PESs used in the $J$-shifting approximation.

| PES | $OH_2$ | OHD | ODH | $OD_2$ |
|---|---|---|---|---|
| $^3A''$ | 3.154 | 1.897 | 2.661 | 1.740 |
| $^3A'$ | 3.127 | 1.884 | 2.631 | 1.725 |

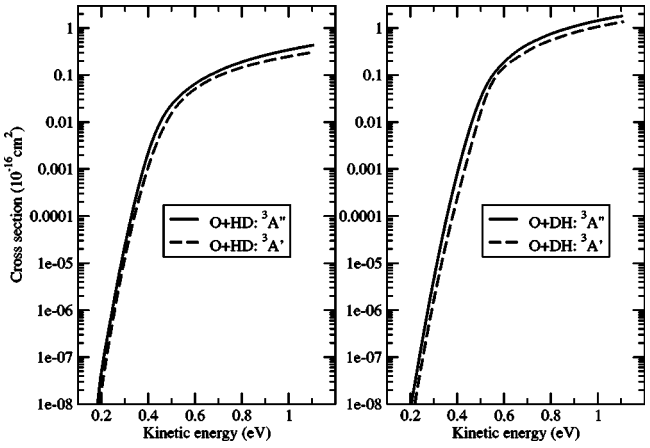


FIG. 3. Initial-state-selected reaction cross sections $\sigma_{vj}(E_{\mathrm{kin}})$ of O+HD $\rightarrow$OH+D and O+DH$\rightarrow$OD+H reactions on $^3A'$ and $^3A''$ PESs as functions of the kinetic energy.

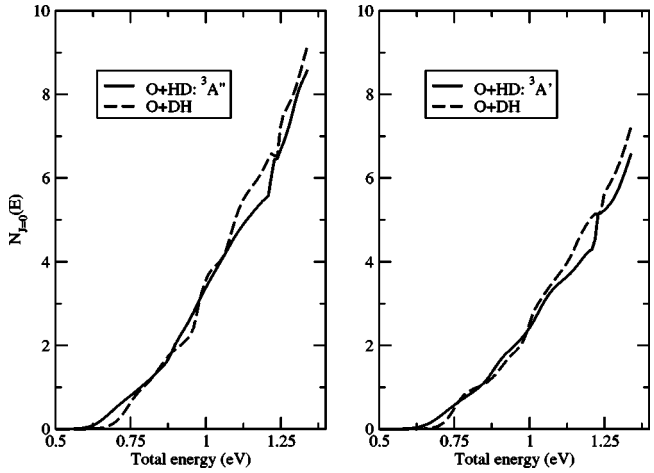


FIG. 4. Cumulative reaction probabilities for O+HD$\rightarrow$OH+D and O+DH$\rightarrow$OD+H reactions for $J=0$ on the $^3A''$ (left panel) and $^3A'$ (right panel) PESs.

The initial-state-selected rate coefficients are not appropriate to compare with experimental measurements because experiments include a thermal population of rotational levels. Thermal rate coefficients are computed from the CRPs. Cumulative reaction probabilities for the two product channels for $J=0$ obtained using the two PESs are shown in Fig. 4. Thermal rate coefficients evaluated from CRP using the $J$-shifting approximation are shown in Fig. 5 for the OH and OD product channels. For comparison, we also include results of Joseph, Truhlar, and Garrett[7] and Garrett and Truhlar[4] for the two branches obtained using variational transition-state calculations. It is seen that the agreement between the different results is quite good for both channels though at higher temperatures the present calculations predict slightly smaller rate coefficients. Numerical values of the thermal rate coefficients for the two channels are given in Table III.

Figure 6 shows the branching ratios between the OH and OD products as functions of the temperature in the range $T=200-600$ K along with the experimental data of Robie *et al.*[9] and theoretical results of Joseph, Truhlar, and Garrett[7] and Garrett and Truhlar.[4] It is seen that the theoretical and experimental results agree with each other for temperatures above 350 K but they differ significantly for $T<350$ K. The rapid increase in the KIE for temperatures lower than 350 K is not reproduced by any of the theoretical results though they employ different potential surfaces and numerical methods. Robie *et al.*[9] attributed the discrepancy between the experiment and available theoretical results to inaccuracies in the potential. The present calculations employ chemically accurate potential energy surfaces and quantum mechanical treatment for the calculations of the rate coefficients. Thus, we do not believe that the discrepancy between theory and experiment is due to inaccuracies in the potential or approximations in the dynamics calculations. The experimental determination of the branching ratio by Robie *et al.*[6,9] makes use of rate coefficients for $O+H_2$ and $O+D_2$ reactions and laser-induced fluorescence (LIF) signals from OH and OD products in $O+H_2$, $O+D_2$, and O+HD reactions,

$$\frac{k_{\mathrm{HD}}}{k_{\mathrm{DH}}}=\frac{k_{\mathrm{H_2}}P_{\mathrm{H_2}}S_{\mathrm{HD}}(\mathrm{OH})S_{\mathrm{D_2}}(\mathrm{OD})}{k_{\mathrm{D_2}}P_{\mathrm{D_2}}S_{\mathrm{DH}}(\mathrm{OD})S_{\mathrm{H_2}}(\mathrm{OH})} \tag{14}$$

TABLE II. Initial-state-selected rate coefficients $k_{v=0,j=0}(T)$ (cm$^3$ molecule$^{-1}$ s$^{-1}$) for reactions (1) and (2).

| $T$ (K) | O+HD$\rightarrow$OH+D | O+DH$\rightarrow$OD+H |
|---|---|---|
| 200.00 | 7.42(−22)[a] | 1.75(−22) |
| 250.00 | 2.46(−20) | 7.98(−21) |
| 300.00 | 3.45(−19) | 1.67(−19) |
| 350.00 | 2.65(−18) | 1.79(−18) |
| 400.00 | 1.32(−17) | 1.18(−17) |
| 450.00 | 4.86(−17) | 5.44(−17) |
| 500.00 | 1.43(−16) | 1.91(−16) |
| 600.00 | 7.65(−16) | 1.33(−15) |
| 700.00 | 2.68(−15) | 5.54(−15) |
| 800.00 | 7.07(−15) | 1.65(−14) |
| 900.00 | 1.54(−14) | 3.92(−14) |
| 1000.00 | 2.91(−14) | 7.89(−14) |

[a]Numbers in parentheses are powers of 10.

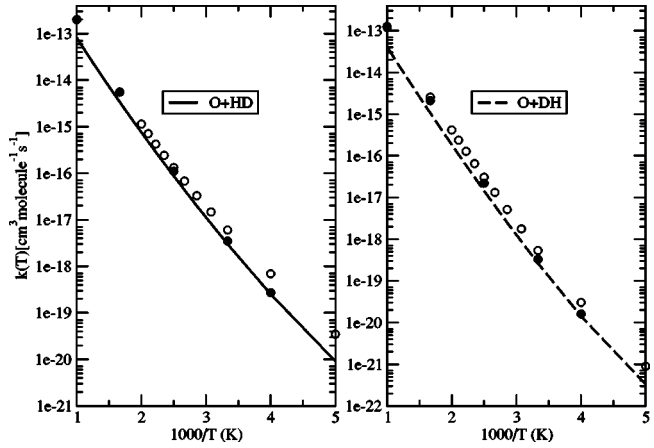


FIG. 5. Thermal rate coefficients for O+HD$\rightarrow$OH+D and O+DH$\rightarrow$OD+H reactions as functions of the temperature: solid curve—present results; filled circles—Joseph, Truhlar, and Garrett (Ref. 7); open circles—Garrett and Truhlar (Ref. 4).

TABLE III. Thermal rate coefficients $k_{HD}(T)$ and $k_{DH}(T)$ ($cm^3$ $molecule^{-1}$ $s^{-1}$) for reactions (1) and (2).

| | $O+DH\rightarrow OD+H$ | | | $O+HD\rightarrow OH+D$ | | |
|---|---|---|---|---|---|---|
| $T$ (K) | $k_{A''}$ | $k_{A'}$ | $k_{DH}=k_{A''}+k_{A'}$ | $k_{A''}$ | $k_{A'}$ | $k_{HD}=k_{A''}+k_{A'}$ |
| 200.00 | 2.53(−22)[a] | 8.73(−23) | 3.40(−22) | 6.40(−21) | 2.72(−21) | 9.12(−21) |
| 250.00 | 1.02(−20) | 4.00(−21) | 1.42(−20) | 1.75(−19) | 7.64(−20) | 2.52(−19) |
| 300.00 | 1.81(−19) | 8.28(−20) | 2.64(−19) | 2.07(−18) | 9.34(−19) | 3.00(−18) |
| 350.00 | 1.64(−18) | 8.52(−19) | 2.49(−18) | 1.35(−17) | 6.37(−18) | 1.99(−17) |
| 400.00 | 9.19(−18) | 5.25(−18) | 1.44(−17) | 5.83(−17) | 2.88(−17) | 8.71(−17) |
| 450.00 | 3.65(−17) | 2.23(−17) | 5.88(−17) | 1.88(−16) | 9.71(−17) | 2.85(−16) |
| 500.00 | 1.13(−16) | 7.21(−17) | 1.85(−16) | 4.91(−16) | 2.63(−16) | 7.54(−16) |
| 600.00 | 6.33(−16) | 4.31(−16) | 1.06(−15) | 2.14(−15) | 1.23(−15) | 3.37(−15) |
| 700.00 | 2.24(−15) | 1.58(−15) | 3.82(−15) | 6.35(−15) | 3.83(−15) | 1.02(−14) |
| 800.00 | 5.88(−15) | 4.26(−15) | 1.01(−14) | 1.47(−14) | 9.20(−15) | 2.38(−14) |
| 1000.00 | 2.36(−14) | 1.75(−14) | 4.11(−14) | 4.92(−14) | 3.27(−14) | 8.19(−14) |

[a]Numbers in parentheses are powers of 10.

where $S_i$ are the LIF signals, $P_{H_2}$ and $P_{D_2}$ are the partial pressures of $H_2$ and $D_2$, and $k_{H_2}$ and $k_{D_2}$ are rate coefficients for the $O+H_2$ and $O+D_2$ reactions. While $k_{H_2}$ was available in the temperature range of $T=297-504$ K, $k_{D_2}$ was available only in the range of $T=416-508$ K and a linear extrapolation of $\ln(k_{D_2})$ versus $1/T$ was used to obtain rate coefficients at lower temperatures. As Joseph, Truhlar, and Garrett[7] pointed out, the accuracy of the Arrhenius fit used to extrapolate the rate coefficients for the $O+D_2$ reaction to low temperatures is questionable. It has been shown[7] that the linear fit is valid only in a limited temperature range. Results for the $O+D_2$ reaction presented in the following section confirm this.

### B. $O(^3P)+D_2$ reaction

Here, we report the quantum mechanical calculations of the $O+D_2$ reaction using the potential surfaces of Rogers *et al.*[19] Since the $J$-shifting approximation works so well for the $O+H_2$ and O+HD cases, we have not attempted to do the full quantum calculation for the $O+D_2$ case. However, we did check the validity of the $J$-shifting approximation by performing calculations for selected values of $J$. A comparison between results of full quantum calculations and the $J$-shifting approximation is given in Fig. 7 where we show cross sections for $J=4$ and $J=6$. It is seen that for both $J$ values, the full quantum and $J$-shifted results are nearly indistinguishable. Thus, we use the $J$-shifting approximation to compute cross sections and rate coefficients.

In Fig. 8 we compare initial-state-selected cross section for the $(v=0,j=0)$ reaction from our calculations on the $^3A''$ potential and the QCT results of Broida and Persky[16] obtained using the potential energy surface of Johnson and Winter.[12] It is seen that the QCT results agree with the quantum results at higher energies but discrepancies occur at lower energies. We have observed similar comparison between the QCT and quantum results for the $O+H_2$ reaction[26] where the QCT results agree with the quantum results at higher energies but show discrepancies at lower energies. The discrepancies are attributed to the differences in the potentials and quantum effects that become important at low energies. The $J=0$ CRP values for the $O+D_2$ reaction are shown in Fig. 9 and thermal rate coefficients derived from the CRPs are given in Fig. 10 along with the theoretical results of Joseph, Truhlar, and Garrett[7] and experimental data of Yang, Shin, and Gardiner[31] and Marshall and Fontijn.[29]

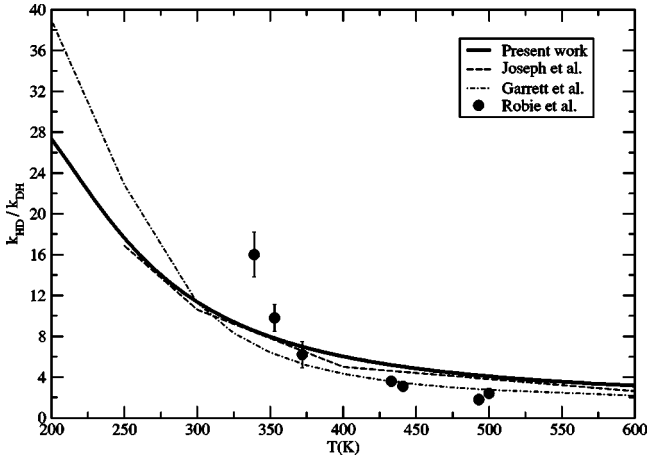


FIG. 6. Branching ratio $k_{HD}/k_{DH}$ as a function of the temperature: solid curve—present results; dashed curve—Joseph, Truhlar, and Garrett (Ref. 7); dot-dashed curve—Garrett and Truhlar (Ref. 1); filled circles—experimental data of Robie *et al.* (Refs. 6 and 9).

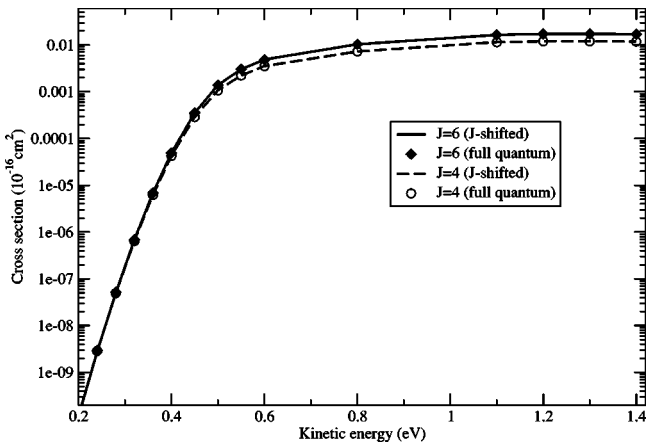


FIG. 7. Comparison of initial-state-selected cross sections for the $O+D_2(v=0,j=0)$ reaction for $J=4$ and $J=6$ from the full quantum calculation and those obtained using the $J$-shifting approximation for collisions occurring on the $^3A''$ PES.

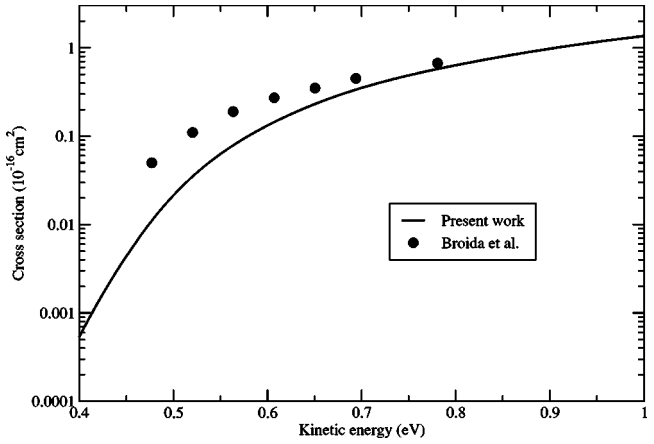


FIG. 8. Initial-state-selected reaction cross sections for the $O+D_2 \rightarrow OD+D$ reaction on the $^3A''$ PES as a function of the translational energy: solid curve—present results; filled circles—Broida and Persky (Ref. 16).

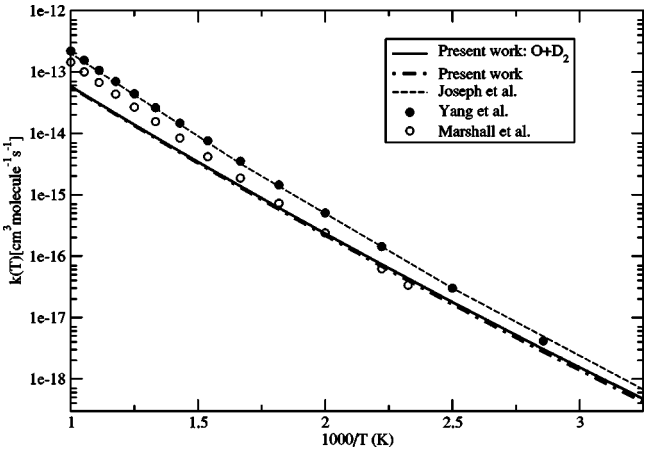


FIG. 10. Thermal rate coefficients for the $O+D_2 \rightarrow OD+D$ reaction as functions of the temperature: solid curve—present results calculated from Eqs. (12) and (13); dot-dashed curve—present results calculated from Eqs. (5) and (8); dashed curve—Joseph, Truhlar, and Garrett (Ref. 7); filled circles—Yang, Shin, and Gardiner (Ref. 31); open circles—Marshall and Fontijn (Ref. 29).

Thermal rate coefficients in the temperature range $T=300-1000$ K are given in Table IV for easy reference.

We have also evaluated thermal rate coefficients using Eq. (8) in which we included a thermal population of rotational and vibrational levels. For temperatures lower than 1000 K converged results are obtained by including $j=0-14$ $(v=0)$ and $j=0-4$ $(v=1)$ in Eq. (8). Each of the $k_{vj}$ were evaluated using the $J$-shifting approximation. Thermal rate coefficients evaluated from Eq. (8) are also shown in Fig. 10 and they are nearly identical to those obtained from CRPs. The overall agreement between the different results is good though the present results agree better with the experimental data of Marshall and Fontijn.[29] At temperatures above 500 K, our results are about a factor of 2 smaller than the experimental data. It is also seen that $\ln k_{D_2}$ versus $1/T$ is not linear and noticeable deviation from linearity occurs for temperatures lower than 500 K.

## IV. CONCLUSIONS

In this paper, we report quantum mechanical investigations of the O+HD and $O+D_2$ reactions. Our calculations employing chemically accurate potential energy surfaces and accurate quantum mechanical treatment of the reaction dynamics fail to account for the rapid increase in $k_{HD}/k_{DH}$ reported in experimental studies by Robie *et al.*[6,9] Our findings are consistent with previous calculations which employed different dynamical methods and potential energy surfaces. The discrepancy between experiment and theory for KIE in O+HD reaction is especially interesting because for the $O+H_2$ reaction quantum calculations[21,25] using the potential energy surfaces employed in the present study were able to quantitatively reproduce cross sections derived from recent crossed molecular beam experiments.[21] Our calculations confirm some doubts on the experimental result cast by Joseph, Truhlar, and Garrett[7] who noted that experimental data may be in error due to extrapolation of the rate coefficient for the $O+D_2$ reaction to low temperatures that were used in obtaining the KIE values. We believe, new measurements could resolve the discrepancy between theory and experiment for this important benchmark reaction.

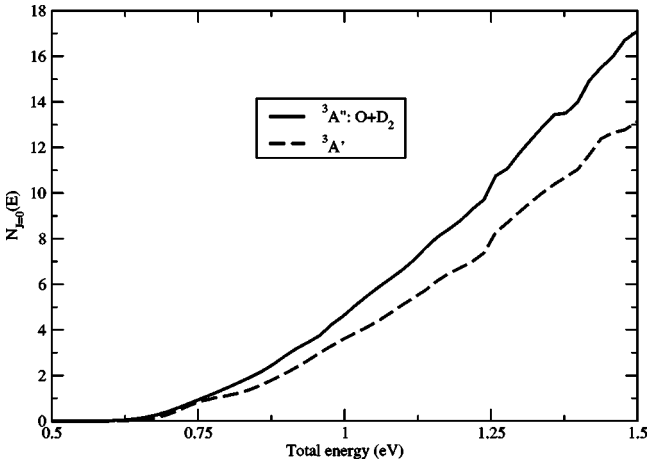


FIG. 9. Cumulative reaction probability of the $O+D_2 \rightarrow OD+D$ reaction for $J=0$ obtained from the $^3A''$ and $^3A'$ PESs.

TABLE IV. Thermal rate coefficient $k_{D_2}(T)$ (cm$^3$ molecule$^{-1}$ s$^{-1}$) for the $O+D_2$ reaction.

| $T$ (K) | $k_{A''}$ | $k_{A'}$ | $k_{D_2}=k_{A''}+k_{A'}$ |
|---|---|---|---|
| 250.00 | 1.17(−20)[a] | 4.44(−21) | 1.61(−20) |
| 300.00 | 2.15(−19) | 1.01(−19) | 3.16(−19) |
| 350.00 | 1.98(−18) | 1.05(−18) | 3.03(−18) |
| 400.00 | 1.13(−17) | 6.50(−18) | 1.78(−17) |
| 450.00 | 4.53(−17) | 2.79(−17) | 7.32(−17) |
| 500.00 | 1.41(−16) | 9.15(−17) | 2.33(−16) |
| 600.00 | 8.18(−16) | 5.65(−16) | 1.38(−15) |
| 700.00 | 2.97(−15) | 2.14(−15) | 5.11(−15) |
| 800.00 | 8.02(−15) | 5.90(−15) | 1.39(−14) |
| 900.00 | 1.76(−14) | 1.32(−14) | 3.08(−14) |
| 1000.00 | 3.35(−14) | 2.54(−14) | 5.89(−14) |

[a]Numbers in parentheses are powers of 10.

## ACKNOWLEDGMENTS

This work was supported by the National Science Foundation through Grant No. ATM-0205199 and the UNLV Planning and Initiative Award.

[1] B. C. Garrett and D. G. Truhlar, Int. J. Quantum Chem. **29**, 1463 (1986).
[2] B. C. Garrett, D. G. Truhlar, and G. C. Schatz, J. Am. Chem. Soc. **108**, 2876 (1986).
[3] B. C. Garrett, D. G. Truhlar, J. M. Bowman, A. F. Wagner, D. Robie, S. Arepalli, N. Presser, and R. J. Gordon, J. Am. Chem. Soc. **108**, 3515 (1986).
[4] B. C. Garrett and D. G. Truhlar, Int. J. Quantum Chem. **31**, 17 (1987).
[5] A. F. Wagner and J. M. Bowman, J. Chem. Phys. **86**, 1976 (1987).
[6] D. C. Robie, S. Arepalli, N. Presser, T. Kitsopoulos, and R. J. Gordon, Chem. Phys. Lett. **134**, 579 (1987).
[7] T. Joseph, D. G. Truhlar, and B. C. Garrett, J. Chem. Phys. **88**, 6982 (1988).
[8] Y. F. Zhu, S. Arepalli, and R. J. Gordon, J. Chem. Phys. **90**, 183 (1989).
[9] D. C. Robie, S. Arepalli, N. Presser, T. Kitsopoulos, and R. J. Gordon, J. Chem. Phys. **92**, 7382 (1990).
[10] P. N. Day and D. G. Truhlar, J. Chem. Phys. **95**, 5097 (1991).
[11] M. Nakamura, J. Chem. Phys. **96**, 2724 (1992).
[12] B. R. Johnson and N. W. Winter, J. Chem. Phys. **66**, 4116 (1977).
[13] D. C. Clary, J. N. L. Connor, and C. J. Edge, Chem. Phys. Lett. **68**, 154 (1979).
[14] G. C. Schatz, A. F. Wagner, S. P. Walch, and J. M. Bowman, J. Chem. Phys. **74**, 4984 (1981).
[15] J. M. Bowman, A. F. Wagner, S. P. Walch, and T. H. Dunning, Jr., J. Chem. Phys. **81**, 1739 (1984).
[16] M. Broida and A. Persky, J. Chem. Phys. **80**, 3687 (1984).
[17] G. C. Schatz, J. Chem. Phys. **83**, 5677 (1985).
[18] D. C. Chatfield, R. S. Friedman, G. C. Lynch, D. G. Truhlar, and D. W. Schwenke, J. Chem. Phys. **98**, 342 (1993).
[19] S. Rogers, D. Wang, A. Kupperman, and S. Walch, J. Phys. Chem. A **104**, 2308 (2000).
[20] M. R. Hoffmann and G. C. Schatz, J. Chem. Phys. **113**, 9456 (2000).
[21] D. J. Garton, T. K. Minton, B. Maiti, D. Troya, and G. C. Schatz, J. Chem. Phys. **118**, 1585 (2003).
[22] N. Balakrishnan, J. Chem. Phys. **119**, 195 (2003).
[23] B. Maiti and G. C. Schatz, J. Chem. Phys. **119**, 12360 (2003).
[24] M. Braunstein, S. Adler-Golden, B. Maiti, and G. C. Schatz, J. Chem. Phys. **120**, 4316 (2004).
[25] N. Balakrishnan, Geophys. Res. Lett. **31**, L04106 (2004).
[26] N. Balakrishnan, J. Chem. Phys. **121**, 6346 (2004).
[27] N. Cohen and K. R. Westberg, J. Phys. Chem. Ref. Data **12**, 531 (1983).
[28] N. Presser and R. J. Gordon, J. Chem. Phys. **82**, 1291 (1985).
[29] P. Marshall and A. Fontijn, J. Chem. Phys. **87**, 6988 (1987).
[30] D. L. Baulch, C. J. Cobos, R. A. Cox *et al.*, J. Phys. Chem. Ref. Data **21**, 411 (1992).
[31] H.-X. Yang, K. S. Shin, and W. Gardiner, Chem. Phys. Lett. **207**, 69 (1993).
[32] L. M. Reynard and D. J. Donaldson, Geophys. Res. Lett. **28**, 2157 (2001).
[33] D. Scouteris, J. F. Castillo, and D. E. Manolopoulos, Comput. Phys. Commun. **133**, 128 (2000).
[34] J. M. Bowman, J. Phys. Chem. **95**, 4960 (1991).
[35] W. H. Miller, J. Chem. Phys. **62**, 1899 (1975).
[36] W. H. Miller, S. D. Schwartz, and J. W. Tromp, J. Chem. Phys. **79**, 4889 (1983).